Eur. J. Biochem. 243, 393–399 (1997)

An ultracentrifugal approach to quantitative characterization of the molecular assembly of a physiological electron-transfer complex

The interaction of electron-transferring flavoprotein with trimethylamine dehydrogenase

Emma K. WILSON[1], Nigel S. SCRUTTON[1], Helmut CÖLFEN[2,3], Stephen E. HARDING[2], Michael P. JACOBSEN[4] and Donald J. WINZOR[4]

[1] Department of Biochemistry, University of Leicester, Leicester, UK
[2] National Centre for Macromolecular Hydrodynamics, University of Nottingham, Sutton Bonington, UK
[3] Department of Colloid Chemistry, Max-Planck-Institute for Colloid and Interface Research, Teltow, Germany
[4] Centre for Protein Structure, Function and Engineering, Department of Biochemistry, University of Queensland, Brisbane, Australia

(Received 21 October 1996) – EJB 96 1545/3

The interaction between two physiological redox partners, trimethylamine dehydrogenase and electron-transferring flavoprotein, has been characterized quantitatively by analytical ultracentrifugation at 4 °C. Analysis of sedimentation-equilibrium distributions obtained at 15000 rpm for mixtures in 10 mM potassium phosphate, pH 7.5, by means of the psi function [Wills, P. R., Jacobsen, M. P. & Winzor, D. J. (1996) *Biopolymers 38*, 119–130] has yielded an intrinsic dissociation constant of 3–7 μM for the interaction of electron-transferring flavoprotein with two equivalent and independent sites on the homodimeric enzyme. This investigation indicates the potential of sedimentation equilibrium for the quantitative characterization of interactions between dissimilar macromolecules.

Keywords: electron-transfer flavoprotein; trimethylamine dehydrogenase; protein interaction; analytical ultracentrifugation.

The coexistence of protein · protein complexes in dissociation equilibrium with their constitutive reactants is a general feature of interprotein-electron-transfer reactions. Whereas the specific interactions involved in the formation of tightly bound protein · protein complexes may be elucidated by NMR and X-ray–crystallographic procedures, those responsible for the weaker electron-transfer complexes are poorly understood because of the inability of current structure-determination procedures to accommodate the lability of the weaker protein · protein complexes. It is thought that the components of the electron-transfer complex may associate initially in unreactive configurations via non-specific interactions, and undergo a diffusional search for the specific configuration commensurate with electron transfer, termed the speculative reduction-in-dimensionality principle. The relatively weak interaction between two physiological redox partners, trimethylamine (Me_3N) dehydrogenase and its electron-transferring flavoprotein (ETF), forms an archetypal example that is an excellent model for studying interprotein electron transfer.

Me_3N dehydrogenase is a complex iron-sulfur flavoprotein that converts Me_3N to dimethylamine and formaldehyde via the reaction [1]

$$(CH_3)_3N + H_2O \rightarrow (CH_3)_2NH + HCHO + 2e^- + 2H^+.$$

In vivo, the electrons derived from this conversion are passed to ETF, thereby generating the oxidised form of the enzyme [2]. Both components of this redox system have been cloned and overexpressed [3, 4], and a high-resolution structure for Me_3N dehydrogenase has been described [5]. A structure for ETF is still awaited [6], but is known to be a heterodimer with polypeptide subunits of M_r 28900 and 33700. Me_3N dehydrogenase is a symmetrical dimer of subunits (M_r 81623 each) in which each subunit contains a single [4Fe-4S] centre [7] and one FMN prosthetic group attached to the protein by a unique 6*S*-cysteinylFMN bond [8, 9]. Removal of the 6*S*-cysteinylFMN bond does not render the enzyme inactive [10], but the detailed catalytic consequences of its removal remain to be determined. The enzyme also binds ADP, but the function of this cofactor remains obscure [11, 12]. The homodimeric enzyme contains a β/α barrel domain at the N-terminus of each subunit, this being the region in which the active site resides. In terms of folding, the C-terminal domains resemble the dinucleotide-binding domains found, for example, in glutathione reductase. A buried loop contains the iron-sulfur centre, which is positioned at the boundary between the N-terminal and C-terminal domains.

From the high-resolution structure of Me_3N dehydrogenase [5] and kinetic analysis of wild-type and mutant proteins [13], a tentative ETF-docking site has been identified on each subunit of Me_3N dehydrogenase. A detailed study of electron transfer from reduced Me_3N dehydrogenase to ETF [14] has yielded a kinetically determined dissociation constant for the protein-protein interaction, but has not taken explicit account of the homodimeric state of Me_3N dehydrogenase. This investigation exploits analytical ultracentrifugation to measure the intrinsic dissociation constant [15] for the interaction of ETF with two equivalent and independent sites on Me_3N dehydrogenase. The present demonstration of the potential of sedimentation-equilibrium studies for the quantitative characterization of electron-transfer-complex formation augurs well for corresponding studies of the assembly of Me_3N dehydrogenase · ETF com-

Correspondence to N. S. Scrutton, Department of Biochemistry, University of Leicester, Leicester LE1 7RH, UK
Fax: +44 116 252 3369.
E-mail: nss4@le.ac.uk

Abbreviations. ETF, electron-transferring flavoprotein; Me_3N, trimethylamine dehydrogenase.

plexes from mutant forms of the two physiological redox partners.

MATERIALS AND METHODS

Preparation of reactants. Me_3N dehydrogenase was purified from *Methylophilus methylotrophus* (bacterium W_3A_1) as described by Steenkamp and Mallinson [1], except that the last gel-filtration step was replaced by chromatography on phenyl-Sepharose [10]. ETF was also obtained from *M. methylotrophus* as described by Steenkamp and Gallup [2], except that gel chromatography was performed on Sephacryl S-100-HR instead of Sephadex G-100, and 1 mM phenylmethylsulfonyl fluoride was included throughout the preparation to suppress proteolysis.

Preparation of reactant solutions. Prior to analytical-ultracentrifuge experiments, the Me_3N dehydrogenase and ETF preparations were dialyzed exhaustively against 10 mM potassium phosphate, pH 7.5, *I* 0.027. Concentrations of Me_3N dehydrogenase solutions were based on a molar extinction coefficient (ε) of 27.3 mM^{-1} cm^{-1} at 443 nm for the subunit [16], and those of ETF on an extinction coefficient of 11.3 mM^{-1} cm^{-1} at 438 nm after oxidation with ferricyanide [2]. From the absorbances of solutions with concentrations determined on the above bases, the absorption coefficients at 280 nm (the wavelength used in the ultracentrifugal study) were as follows: ε_{280} = 66.1 mM^{-1} cm^{-1} for ETF; ε_{280} = 404 mM^{-1} cm^{-1} for the Me_3N dehydrogenase homodimer.

Sedimentation-equilibrium studies. The separate reactants, and mixtures thereof, were subjected to sedimentation equilibrium at 4 °C in a Beckman XL-A analytical ultracentrifuge. Rotor speeds of 10000 rpm and 17000 rpm were used in the respective experiments on Me_3N dehydrogenase and ETF, whereas mixtures were centrifuged at 15000 rpm. Equilibrium distributions were recorded spectrophotometrically at 280 nm, and the baseline determined at the end of each experiment by increasing the rotor speed to pellet all protein. The loading concentration of ETF was maintained at 0.5 mg/ml in all reaction mixtures, whereas that of Me_3N dehydrogenase ranged between 0.7 mg/ml and 2.0 mg/ml.

Psi analysis of sedimentation-equilibrium distributions. The sedimentation-equilibrium distributions were analyzed directly by expressing the total absorbance, $A_t(r)$, at radial distance r as

$$A_t(r) = A_A(r) + A_S(r) + A_{AS}(r) + A_{AS2}(r) \qquad \text{Eqn 1}$$

where the absorbances of AS and AS_2 at each radial distance must also be related to those of free A and S by the law of mass action describing the chemical equilibria, an aspect that is taken into account later. Advantage is taken of the basic sedimentation-equilibrium equation, which allows the thermodynamic activity of a solute species, $a_i(r)$, at any radial distance r to be expressed in terms of that, $a_i(r_F)$, at some fixed radial distance r_F as [17, 18]

$$a_i(r) = a_i(r_F)\exp[M_{ri}(1-\bar{v}_i\varrho)\omega^2(r^2-r_F^2)/2RT] \qquad \text{Eqn 2}$$

where ω is the angular velocity in an experiment conducted at temperature T, and R is the universal gas constant. M_{ri} is the relative molecular mass of species i and $\bar{v}_i$ its partial specific volume, and ϱ is the solvent density [19]. Because of the identity of concentrations and thermodynamic activities for (assumed) ideal solution behaviour and the proportionality between absorbance and concentration, Eqn 1 may be written in the form

$$A_t(r) = A_A(r_F)\psi_A(r) + A_S(r_F)\psi_S(r) + A_{AS}(r_F)\psi_{AS}(r) + A_{AS2}(r_F)\psi_{AS2}(r) \qquad \text{Eqn 3a}$$

where the psi function $\psi_i(r)$, defined as

$$\psi_i(r) = \exp[M_{ri}(1-\bar{v}_i\varrho)\omega^2(r^2-r_F^2)/2RT] \qquad \text{Eqn 3b}$$

has been introduced [20] as a parameter to express the consequences of sedimentation-equilibrium requirements. Although the psi function is a transformed variable, the virtual lack of uncertainty in measurements of radial distance renders irrelevant the usual concern about distortion of error by such transformation [21].

For the present system, it is convenient to write Eqn 3a in the form

$$A_t(r)/\psi_S(r) = A_S(r_F) + A_A(r_F)[\psi_A(r)/\psi_S(r)] + A_{AS}(r_F)[\psi_{AS}(r)/\psi_S(r)] + ... \qquad \text{Eqn 4}$$

which signifies that the dependence of $A_t(r)/\psi_S(r)$ upon $\psi_A(r)/\psi_S(r)$ has an ordinate intercept of $A_S(r_F)$ and a limiting initial slope of $A_A(r_F)$. The potential utility of this means of evaluating the two parameters in this manner is examined later. In the application of Eqn 4 to sedimentation-equilibrium distributions for mixtures of ETF (S) and Me_3N dehydrogenase (A), the magnitudes of $\psi_S(r)$ and $\psi_A(r)$ were calculated on the basis of partial specific volumes of 0.738 ml/g for ETF [22] and 0.731 ml/g for Me_3N dehydrogenase [23]: relative molecular masses were taken as those of the heterodimer (63500) and homodimer (163000) for S and A respectively.

To cover the possibility that the slope of the required limiting tangent may be difficult to define experimentally, $A_A(r_F)$ has been determined by the analog of an earlier direct analysis of sedimentation-equilibrium distributions [24]. The value of $A_S(r)$, calculated as $A_S(r_F)\psi_S(r)$ in accordance with Eqns 2 and 3, was subtracted from the corresponding total absorbance at each radial distance to obtain a revised sedimentation-equilibrium distribution with A (Me_3N dehydrogenase) as the smallest macromolecular species. The counterpart of Eqn 4 for this revised distribution, namely,

$$[A_t(r)-A_S(r)]/\psi_A(r) = A_A(r_F) + A_{AS}(r_F)[\psi_{AS}(r)/\psi_A(r)] + A_{AS2}(r_F)[\psi_{AS2}(r)/\psi_A(r)] \qquad \text{Eqn 5}$$

has allowed a second estimate of $A_A(r_F)$ to be obtained as the ordinate intercept of the dependence of $[A_t(r)-A_S(r)]/\psi_A(r)$ upon $[\psi_{AS}(r)/\psi_A(r)]$.

Evaluation of $A_S(r_F)$ and $A_A(r_F)$ by such means allowed delineation of the respective absorbance distributions for free ligand and free acceptor as $A_S(r_F)\psi_S(r)$ and $A_A(r_F)\psi_A(r)$, which were converted to molar concentration distributions, $c_i(r)$, by means of the absorption coefficients reported above. The residual absorbance at each radial distance r, namely, $\Delta A_t(r) = A_t(r) - A_S(r) - A_A(r)$, reflects the combined absorbances of acceptor · ligand complexes, and has therefore been analyzed in terms of the expression

$$\Delta A_t(r) = 2K\varepsilon_{AS}c_A(r)c_S(r) + K^2\varepsilon_{AS2}\,c_A(r)[c_S(r)]^2 \qquad \text{Eqn 6}$$

where K is the intrinsic association constant [15] for the interaction of ETF with two equivalent and independent sites on the Me_3N dehydrogenase homodimer. Absorption coefficients of 235000 M^{-1} cm^{-1} and 179000 M^{-1} cm^{-1} were calculated for AS and AS_2, respectively, by combining those for Me_3N dehydrogenase and ETF with the stoichiometry of complex formation: $\varepsilon_{AS} = (\varepsilon_A + \varepsilon_S)/2$ and $\varepsilon_{AS2} = (\varepsilon_A + 2\varepsilon_S)/3$.

The intrinsic binding constant was therefore obtained by non-linear-regression analysis in terms of the relationship

$$\Delta A_t(r)/c_A(r) = 2K\varepsilon_{AS}c_S(r) + K^2\varepsilon_{AS2}[c_S(r)]^2 \qquad \text{Eqn 7}$$

wherein the left-hand side is fitted to the single independent variable $c_S(r)$.

Numerical simulation of sedimentation-equilibrium distributions. Equilibrium distributions were generated for systems

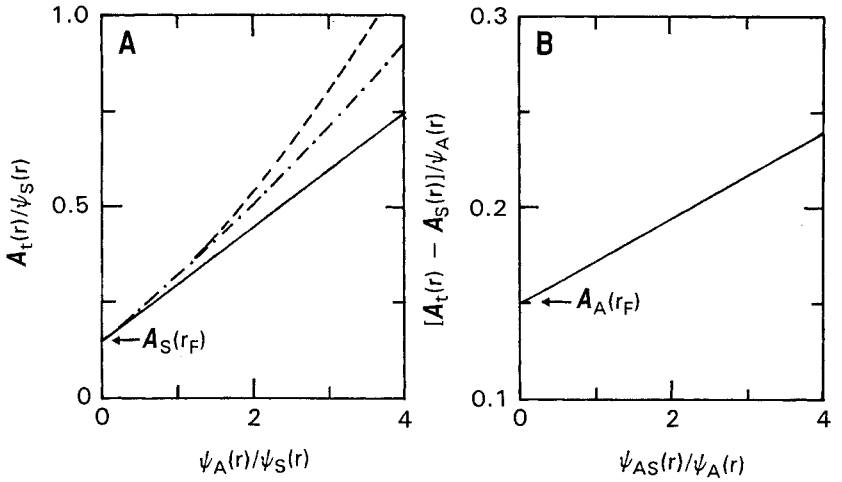

Fig. 1. Illustration of the psi procedure for determining the free concentrations (absorbances at 280 nm) of free acceptor and ligand by its application to simulated sedimentation-equilibrium distributions. (a) Analysis of data for systems with M_{rS} = 50000 and M_{rA} = 100000 (– – –) or M_{rA} = 150000 (– · – · –) according to Eqn (4) to assess the feasibility of determining $A_S(r_F)$ and $A_A(r_F)$ as the ordinate intercept and limiting slope, respectively. The solid line denotes the theoretical limiting slope in these simulated experiments at 4 °C and 15000 rpm. (b) Alternative estimation of $A_A(r_F)$ by analysis of a revised absorbance distribution in terms of Eqn (8).

involving reversible 1:1 complex formation between a ligand (M_{rS} = 50000) and an acceptor (M_{rA} = 150000 or 100000) subjected to ultracentrifugation at 15000 rpm at 4 °C. The radial extremities of the liquid column were taken as 6.90 cm and 7.20 cm, and the column midpoint was selected as the reference radial position (r_F = 7.05 cm). After assigning magnitudes to $c_A(r_F)$ and $c_S(r_F)$, the equilibrium distributions of the free reactants were generated via Eqn 2 on the basis of a value of 0.25 for $(1-v_A\varrho)$ and $(1-v_S\varrho)$. Chemical equilibrium was ensured by making $c_{AS}(r_F)$ equal to the product of $c_A(r_F)$, $c_S(r_F)$ and the association constant K, which was taken as 10^5 M^{-1}. Eqn 2 was used to define the concentration of complex throughout the equilibrium distribution. The three concentration distributions were converted to their absorbance counterparts by assigning a common molar absorption coefficient of 10^5 M^{-1} cm^{-1} to all species, after which the equilibrium distribution in terms of $A_t(r)$ was obtained as the sum of the three absorbance contributions at each radial distance.

RESULTS

Although use of the psi function for the characterization of solute interactions is a recent development [20], the direct analysis of sedimentation-equilibrium distributions for such purposes is not. However, because the omega procedure [18, 24], from which the psi analysis evolved, has had such little impact north of the equator, it is appropriate to illustrate the application of the present approach to simulated sedimentation-equilibrium distributions of reversible 1:1 complex formation between two dissimilar macromolecular reactants.

Illustrative application of the psi analysis to simulated equilibrium distributions. The application of Eqn 4 to simulated diistributions is illustrated in Fig. 1a, which refers to data generated on the basis of a rotor speed of 15000 rpm and a temperature of 4 °C to comply with the experimental study of ETF. A value of 50000 was assigned to M_{rS}, while the relative molecular mass of the acceptor has been taken as either 150000 (– · – · –) or 100000 (– – –). The patterns have been generated in such a manner that $A_S(r_F) = A_A(r_F) = 0.15$. Although these two dependences of $A_t(r)/\psi_S(r)$ upon $\psi_A(r)/\psi_S(r)$ yield a common ordinate intercept that coincides with that of the theoretical limiting tangent $A_s(r_F)$, their limiting slopes [as $\psi_A(r)/\psi_S(r)$ tends to 0] diverge slightly from the theoretical value. Consequently, even though reasonably accurate definition of a limiting tangent may ensue from such analysis of an experimental sedimentation-equilibrium distribution, caution should be exercized in assigning a magnitude to $A_A(r_F)$ on the basis of its slope. The extent of overestimation of this parameter by such means is likely to vary inversely with the size difference between acceptor and ligand, and with rotor speed. The optimal situation would entail the selection of a rotor speed that rendered the experiment a low-speed run [25] from the viewpoint of the distribution of free S but a run of meniscus-depletion design [26] for A and AS complex(es). However, irrespective of the uncertainty that surrounds the evaluation of $A_A(r_F)$ by this means, the analysis of the total absorbance distribution according to Eqn 4 should provide an acceptable estimate of $A_S(r_F)$, which is an important consideration because knowledge of this parameter and hence of $A_S(r)$ throughout the distribution is a prerequisite for determination of $A_A(r_F)$ by the suggested alternative procedure.

The application of Eqn 5 to the revised sedimentation-equilibrium distribution that results from subtraction of $A_S(r)$ is shown in Fig. 1b. Consistent with the theoretical requirements of Eqn 4 for a system restricted to 1:1 complex formation [$A_{AS2}(r_F)$ = 0], the plots for the two systems are coincident and linear, with an ordinate intercept and slope that define the magnitudes of $A_A(r_F)$ and $A_{AS}(r_F)$, respectively. Upward curvature of this secondary plot would signify the existence of a contribution to $[A_t(r)-A_S(r)]/\psi_A(r)$ from higher-order complexes, i.e. the AS_2 term in Eqn 5 and the higher-order terms if the multivalence of A is greater than 2. Thus, whereas the curvilinear form of the plots in the primary psi analysis (Fig. 1a) merely confirms the equilibrium coexistence of A and S in free and complexed states, a curvilinear secondary plot signifies the existence of complexes with greater than 1:1 stoichiometry.

In summary, these analyses of simulated sedimentation-equilibrium distributions have served two major purposes. First, they have identified a potential experimental problem with the determination of $A_A(r_F)$ from the slope of the primary plot (Fig. 1a), but have supported the theoretical prediction that a reasonable estimate of $A_S(r_F)$ should emanate from this analysis of the total absorbance distribution in accordance with Eqn 4. Secondly, they have indicated the feasibility of using an alternative analy-

sis for the evaluation of $A_A(r_F)$. This alternative procedure, based on Eqn 5, employs the magnitude of $A_S(r_F)$ evaluated from the primary analysis to allow calculation of a revised absorbance distribution in which acceptor (A) becomes the smallest macromolecular species. Both analyses originate from the corresponding treatment of sedimentation-equilibrium distributions in terms of the omega function [24, 27].

Macromolecular states of the two reactants. Characterization of Me_3N dehydrogenase by analytical ultracentrifugation under the present conditions (pH 7.5, *I* 0.027) has confirmed an earlier conclusion [23], based on studies at higher ionic strength (pH 7.5, *I* 0.1), that Me_3N dehydrogenase exists in solution as the homodimer (M_r = 163000), which is consistent with the X-ray–crystallographic structure of the enzyme [5]. Corresponding studies with ETF [22] have established the existence of this flavoprotein as a heterodimer (M_r = 63500) that coexists in equilibrium with its two dissimilar subunits. The magnitude of the association constant (40 l/g) under the present conditions is such that consideration needs to be given to this dissociation of ETF in reaction mixtures with Me_3N dehydrogenase.

Psi analysis of sedimentation-equilibrium distributions for Me_3N dehydrogenase/ETF mixtures. To accommodate the consequences of ETF dissociation on the proposed treatment of distributions for mixtures of ETF and Me_3N dehydrogenase, Eqn 1 requires an additional term to include the absorbance contribution from monomeric ligand (D). To examine the consequences of including this additional term, we write the counterpart of Eqn 4 as

$$A_t(r)/\psi_T(r) = A_D(r_F) + A_S(r_F)[\psi_S(r)/\psi_D(r)] + A_A(r_F)[\psi_A(r)/\psi_D(r)] + ... \quad \text{Eqn 8}$$

from which it is evident that a plot of $A_t(r)/\psi_D(r)]$ versus $[\psi_S(r)/\psi_D(r)]$ has the potential to yield $A_D(r_F)$ as the ordinate intercept and $A_S(r_F)$ as the limiting initial tangent.

Analyses of sedimentation-equilibrium distributions for mixtures of ETF (0.5 mg/ml) and 0.7 mg/ml or 0.9 mg/ml Me_3N dehydrogenase in terms of Eqn 8 are summarized in Fig. 2a, the corresponding treatment of the same results in accordance with Eqn 4 being presented in Fig. 2b. The former plot cannot provide an accurate estimate of the ordinate intercept, a feature that contrasts markedly with the corresponding dependence of $A_t(r)/\psi_S(r)]$ upon $\psi_A(r)/\psi_S(r)$. If the absorbance contribution by dissociated ETF (D) at the reference radial position were essentially zero, interpretation of Fig. 2b in terms of Eqn 4 would imply that the absorbance contributed by free S to the selected $A_t(r_F)$ of 0.45 is 0.15, a value which should also describe the slope of the limiting initial tangent in Fig. 2a. The required limiting tangent is not defined by the experimental data, which are, however, consistent with the description in terms of a line drawn through the origin with the slope predicted from the intercept of Fig. 2b, even though calculations based on the dimerization constant of 40 l/g [22] indicate the existence of roughly equal proportions of S and D. Analysis of sedimentation-equilibrium distributions in terms of Eqn 4 is therefore considered to suffice for the purpose of defining the free concentration of ETF, whether it be as a heterodimer or subunits thereof.

The same relationship, $A_t(r) = 0.147\ (\pm 0.006) + 0.30\ (\pm 0.01)[\psi_A(r)/\psi_S(r)]$, effectively describes the entire sedimentation-equilibrium distributions obtained for both reaction mixtures. The superimposition of the two sedimentation-equilibrium distributions reflects the essential absence of Me_3N dehydrogenase in the meniscus region and hence the presence of comparable concentrations of this reactant at r_F, which was chosen on the basis of a total absorbance of 0.45 in both experiments. The linearity of Fig. 2b signifies the absence of any significant contribution of Me_3N dehydrogenase · ETF complex(es) to the right-hand side of Eqn 4. In other words, these two results reflect the combined absorbance distributions for a non-interacting mixture of Me_3N dehydrogenase and ETF. Since the magnitude of the ordinate intercept in Fig. 2a should be maximal, inasmuch as complex formation would lead to an even smaller $A_D(r_F)$ in a reacting mixture with the same ETF concentration, we shall employ the counterpart of Fig. 2b for determinations of $A_S(r_F)$ and $A_A(r_F)$ for an interacting mixture.

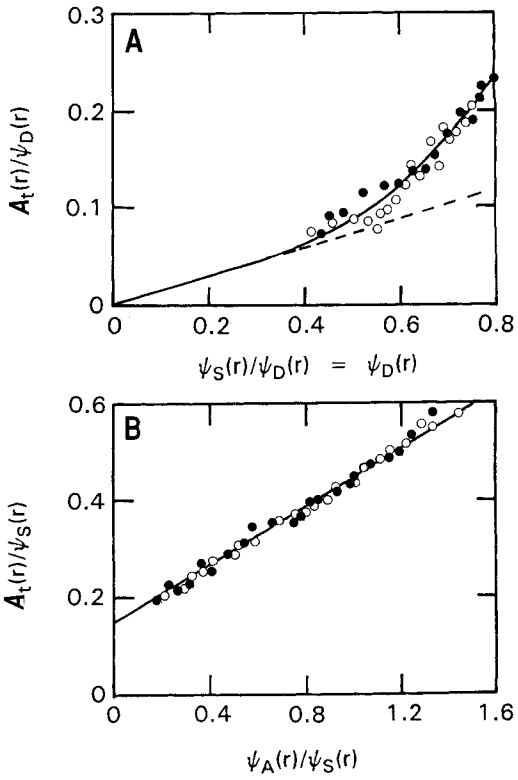

Fig. 2. Search for the consequences of ETF dissociation on the psi analysis for determining the concentrations (absorbances at 280 nm) of free ETF and Me_3N dehydrogenase in mixtures thereof. Data from sedimentation-equilibrium distributions for mixtures (0.5 mg/ml ETF) containing 0.7 mg/ml (○) or 0.9 mg/ml (●) Me_3N dehydrogenase are plotted according to Eqn 8 (a) and Eqn 4 (b) with the reference radial positions (r_F) selected on the basis of a common absorbance, $A_t(r_F)$, of 0.45.

The results of the use of Eqn 4 for analysis of a sedimentation-equilibrium distribution for a mixture with a higher loading concentration of Me_3N dehydrogenase (2 mg/ml) is summarized in Fig. 3a, which implicate the existence of acceptor · ligand complex formation by virtue of its curvilinearity. Least-squares calculations on results in the region $0.4 < \psi_A(r)/\psi_S(r) < 0.7$ yielded the relationship $A_t(r)/\psi_S(r) = 0.130\ (\pm 0.005) + 0.28\ (\pm 0.01)[\psi_A(r)/\psi_S(r)]$ for the initial limiting tangent. Respective values of 0.13 and 0.28 for $A_S(r_F)$ and $A_A(r_F)$ are thus indicated by the ordinate intercept and slope. However, a smaller magnitude for $A_A(r)$ is obtained from the plot (Fig. 3b) of the revised absorbance distribution [after subtraction of $A_S(r)$] in accordance with Eqn 5, for which linear-regression analysis signifies an ordinate intercept of 0.24 (± 0.01). These results thus reinforce the earlier inference that the limiting tangent to the dependence of $A_t(r)/\psi_S(r)$ upon $[\psi_A(r)/\psi_S(r)]$ is likely to overestimate $A_A(r_F)$.

Use of the ordinate intercept from Fig. 3b for $A_A(r_F)$ to calculate the absorbance distribution of free Me_3N dehydrogenase as $A_A(r_F)\psi_A(r)$ allowed the determination of residual absor-

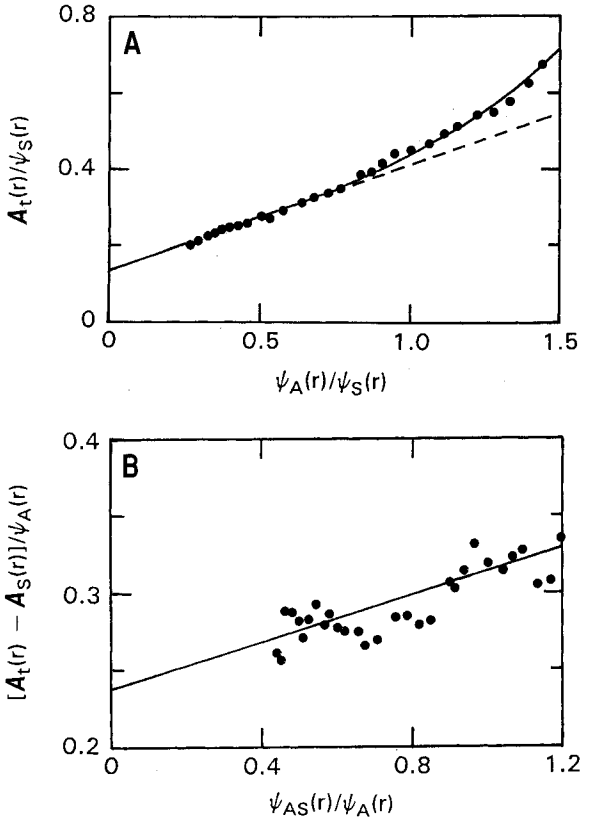

Fig. 3. Determination of the absorbances of free ETF (S) and Me_3N dehydrogenase (A) at the reference radial position from the sedimentation-equilibrium distribution for an interacting mixture of the two reactants in 10 mM sodium phosphate, pH 7.5, at 4°C. (a) Data from the sedimentation-equilibrium distribution for the mixture (0.5 mg/ml ETF, 2.0 mg/ml Me_3N dehydrogenase) according to Eqn (4) with the reference radial position selected to achieve a value of 0.45 for $A_t(r_F)$. $A_S(r_F)$ is given by the ordinate intercept. (b) Secondary plot of the revised absorbance distribution in accordance with Eqn (5) to obtain $A_A(r_F)$ as the ordinate intercept.

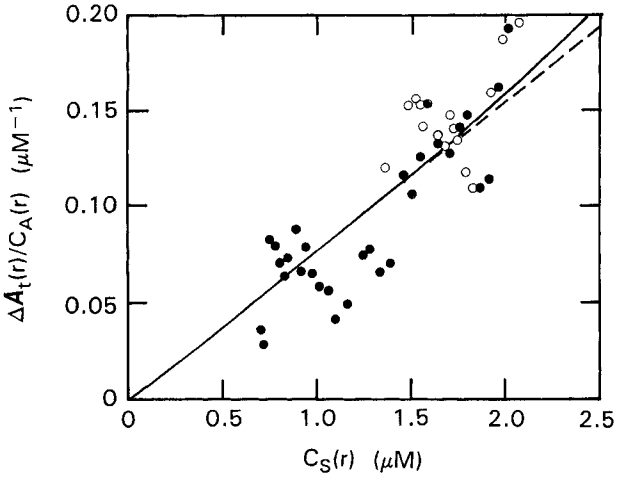

Fig. 4. Quantitative characterization of the Me_3N dehydrogenase · ETF interaction by sedimentation equilibrium in 10 mM sodium phosphate, pH 7.5, at 4°C. Analysis of residual absorbances, $\Delta A_t(r)$, from sedimentation-equilibrium distributions for mixtures containing 0.5 mg/ml ETF and 2.0 mg/ml (●) or 1.7 mg/ml (○) Me_3N dehydrogenase according to Eqn (7) (——) and the corresponding expression for a univalent acceptor (– – –).

bances, $\Delta A_t(r)$, throughout the sedimentation-equilibrium distribution. These residual absorbances are summarized in Fig. 4, together with those from an experiment with 1.7 mg/ml Me_3N dehydrogenase and the best-fit description obtained by non-linear-regression analysis in terms of Eqn 4. On this basis, the interaction of ETF heterodimer with two equivalent and independent sites on Me_3N dehydrogenase is described by an intrinsic association constant of 6.7 (±0.4) μM. In that regard, the results could equally well be construed in terms of ETF interaction with a single site on the Me_3N dehydrogenase homodimer, in which case the best-fit linear relationship would signify a dissociation constant of 3.0 (±0.2) μM. However, the existence of a twofold axis of symmetry in the crystal structure of Me_3N dehydrogenase homodimer [5] is considered to favour interpretation of the results in terms of an intrinsic equilibrium constant for a site on each subunit. Distinction between the two possibilities would require the use of a much greater range of ETF concentrations to enhance the proportion of AS_2 species sufficiently to introduce significant curvilinearity into Figs 3b and 4. The essentially linear form of these two plots signifies the dominance of complex(es) with 1:1 stoichiometry, but does not comment upon the number of ways in which complexes with that stoichiometry have been formed.

Although there is supportive evidence (Fig. 2) for neglect of the effects of ETF dissociation in the elucidation of the absorbance distribution of free ligand via Eqn 4, no justification has been provided for the use of those $A_S(r)$ values to interpret the residual absorbances, $\Delta A_t(r)$, in terms of Eqn 7. The inherent assumption that free ETF exists solely in the heterodimeric state is in conflict with the prediction [22] that ETF should comprise approximately equal concentrations (by mass) of heterodimeric and dissociated states over the $A_S(r)$ range covered in Fig. 4. Because the subunit bearing the potential site for interaction with Me_3N dehydrogenase represents only half of the dissociated material, there is also an equimolar distribution of free ETF between heterodimeric and active subunit states. The possible consequences of ETF dissociation on the interpretation of Fig. 4 need to be addressed.

First we consider the situation in which the affinity of Me_3N dehydrogenase for the ETF subunit bearing the binding site is unaffected by dissociation of the heterodimer. The consequent identity of the intrinsic association constant (K) for either ETF state would render redundant the need to apportion $c_S(r)$ between values for the heterodimeric and dissociated states, because the relevant parameter for use in Eqn 7 would be the summed molar concentrations of the two forms of free ligand, i.e., $c_S(r)$. The above interpretation of Fig. 4 would thus retain validity for this simplest situation involving equivalent and independent binding of the two ligand states.

The second case to be considered is an extreme situation in which Me_3N dehydrogenase only exhibits affinity for the heterodimeric state of ETF. Under those circumstances, the depletion of the concentration of free heterodimer as the result of complex formation would necessarily be countered by association of dissociated ETF to re-establish equilibrium between the two states of free ligand. The net result of such re-equilibration would be maintenance of the ETF distribution between heterodimeric and dissociated states applying to the free ligand concentration in the absence of acceptor (approximately equal proportions in the present instance). This situation is readily reconciled with interpretation of results in terms of Eqn. 7, the only consequential change to which is the replacement of $c_S(r)$ by $Fc_S(r)$, where F is the fraction of free ETF in the heterodimeric state. On the basis that F is about 0.5, the magnitude of K would then be twice the value inferred from Fig. 4. In other words, an intrinsic dissociation constant of 3.3 (±0.2) μM would describe the ex-

clusive binding of ETF heterodimer to two equivalent and independent sites on homodimeric Me_3N dehydrogenase.

Another extreme situation requiring consideration is that in which Me_3N dehydrogenase exhibits no affinity for heterodimeric ETF. Exclusive binding of the relevant dissociated ETF subunit to form Me_3N dehydrogenase · ETF complexes would necessitate re-establishment of the dissociation equilibrium between heterodimeric and dissociated states of free ETF. Provided that interaction between ETF subunits is restricted to heterodimer formation (the possibility favoured by the failure of X-ray studies to obtain evidence of a homodimeric ETF structure), the distribution of free ETF between heterodimeric and dissociated forms would be unaffected by acceptor · ligand-complex formation. Because the fraction of free ETF in the dissociated state $(1-F)$ is 0.5, an intrinsic dissociation constant of 3.3 (± 0.2) μM would describe the exclusive binding of the relevant dissociated ETF subunit to Me_3N dehydrogenase.

An outcome of the above deliberations is that consideration of these three markedly differing situations has led to relatively similar estimates for the magnitude of the intrinsic binding constant for the interaction of ETF with Me_3N dehydrogenase. In the absence of any specific information about the nature of the ETF state involved in physiological electron transfer, we can therefore only invoke an intrinsic dissociation constant of 3–7 μM for the interaction of ETF with two equivalent and independent sites on homodimeric ETF, a range that encompasses the intermediate values that would emanate if Me_3N dehydrogenase were to exhibit preferential, rather than exclusive, affinity for the heterodimeric or dissociated forms of ETF.

DISCUSSION

This investigation of the interaction between Me_3N dehydrogenase and ETF has served two main roles. From the ultracentrifugation viewpoint, this use of the psi function continues interest in the prospect of direct analysis of sedimentation-equilibrium distributions recorded in terms of total solute concentration as a means to characterize interactions between dissimilar macromolecules [24, 27–29], some 20 years after development of the omega analysis [24, 27] from which the present procedure has evolved. In that regard, the present results illustrate the manner in which sedimentation-equilibrium studies can be used to characterize protein-protein interactions, but grossly understate the potential precision and accuracy with which such characterization can be accomplished under more favourable circumstances. A limiting factor in the present study was the necessity to examine the Me_3N dehydrogenase · ETF interaction in a concentration range that was too low for optimal quantification but was the highest commensurate with the optical system available in the new-generation analytical ultracentrifuge. The imminent re-introduction of the Rayleigh interference optical system should restore the precision of sedimentation-equilibrium measurements to that attainable in the older-generation instruments. Fortunately, ambiguity about the macromolecular state of functional ETF in its physiological elecron-transfer role has rendered less important the matter of precision in the present estimates of the dissociation constant by sedimentation equilibrium.

This investigation has contributed to our knowledge of the physiological electron transfer between Me_3N dehydrogenase and ETF. The present results could have been interpreted in terms of a 1:1 interaction and a dissociation constant in the range 1.5–3 μM. However, the emphasis has been placed on their interpretation in terms of ETF interaction with two equivalent and independent binding sites on Me_3N dehydrogenase (dissociation constant of 3–7 μM) to comply with other evidence [5, 7] that the enzyme is a symmetrical homodimer with two [4Fe-4S] centres. It seems reasonable to surmise that the dissociation constants of 10–20 μM obtained by stopped-flow measurements [14] were also intrinsic values for the interaction of ETF with two Me_3N dehydrogenase sites. Although those analyses were based on an expression for a 1:1 interaction [30], it would also accommodate, upon re-identifying the nature of the dissociation constant, equivalence and independence of ligand interactions with a multivalent acceptor.

In summary, the important finding from the viewpoint of electron-transfer-complex assembly is that the results of this ultracentrifugal investigation are compatibile with the existence of two independent and equivalent binding sites for ETF on the surface of Me_3N dehydrogenase. This observation is consistent with published crystallographic data [5] and the refined version thereof (White, S. A. & Mathews, F. S., personal communication), which signify a twofold axis of symmetry in the homodimer. Recent stopped-flow kinetic data on wild-type and mutant complexes (Wilson, E. K., Huang, L., Hille, R. & Scrutton, N. S., unpublished data) signify that Tyr442 is located at the center of the interaction surface of Me_3N dehydrogenase. The precise size of this surface is unknown but is postulated [13] to be as large as 1200 Å^2, the positions of the putative docking sites on the Me_3N dehydrogenase dimer being compatible with bivalent-complex formation. Further studies entailing site-directed mutagenesis of residues in the interaction surface will benefit greatly from the information on reaction stoichiometry provided by ultracentrifugal analysis to supplement the quantitative characterization of complex assembly by stopped-flow kinetics.

This investigation was supported by the Leverhulme Trust (N. S. S.), the Medical Research Council (E. K. W. and N. S. S.), the Royal Society (N. S. S.), the Biotechnology and Biological Sciences Research Council and the Engineering and Physical Sciences Research Council (S. E. H. and H. C.), and the Australian Research Council (D. J. W.).

REFERENCES

1. Steenkamp, D. J. & Mallinson, J. (1976) Trimethylamine dehydrogenase from a methylotrophic bacterium. 1. Isolation and steady-state kinetics, *Biochim. Biophys. Acta 429*, 705–719.
2. Steenkamp, D. J. & Gallup, M. (1978) The natural flavoprotein electron acceptor of trimethylamine dehydrogenase, *J. Biol. Chem. 253*, 4086–4089.
3. Boyd, G., Mathews, F. S., Packman, L. C. & Scrutton, N. S. (1992) Trimethylamine dehydrogenase of bacterium W_3A_1: molecular cloning, sequence determination and overexpression of the gene, *FEBS Lett. 308*, 271–276.
4. Chen, D. W. & Swenson, R. P. (1994) Cloning, sequence analysis, and expression of the genes encoding the two subunits of the methylotrophic bacterium W_3A_1 electron transfer protein, *J. Biol. Chem. 269*, 32120–32128.
5. Lim, L. W., Shamala, N., Mathews, F. S., Steenkamp, D. J., Hamlin, R. & Xuong, N. (1986) Three-dimensional structure of the iron-sulfur flavoprotein trimethylamine dehydrogenase, *J. Biol. Chem. 261*, 15140–15146.
6. White, S. A., Mathews, F. S., Rohlfs, R. J. & Hille, R. (1994) Crystallization and preliminary crystallographic investigation of electron-transfer flavoprotein from the bacterium *Methylotrophilus* W_3A_1, *J. Mol. Biol. 240*, 265–266
7. Hill, C. L., Steenkamp, D. J., Holm, R. H. & Singer, T. P. (1977) Identification of the iron-sulfur center in trimethylamine dehydrogenase, *Proc. Natl Acad. Sci. USA 74*, 547–551.
8. Steenkamp, D. J., McIntire, W. & Kenney, W. C. (1978) Structure of the covalently bound coenzyme of trimethylamine dehydrogenase: evidence for a 6-substituted flavin, *J. Biol. Chem. 253*, 2818–2828.

9. Kenney, W. C., McIntire, W., Steenkamp, D. J. & Benisek, W. F. (1978) Amino acid sequence of a cofactor peptide from trimethylamine dehydrogenase, *FEBS Lett. 85*, 137–140.
10. Scrutton, N. S., Packman, L. C., Mathews, F. S., Rohlfs, R. J. & Hille, R. (1994) Assembly of redox centers in the trimethylamine dehydrogenase of bacterium W_3A_1 properties of the wild-type enzyme and a C30A mutant expressed from a clone gene in *Escherichia coli*, *J. Biol. Chem. 269*, 13942–13950.
11. Lim, L. W., Mathews, F. S. & Steenkamp, D. J. (1988) Identification of ADP in the iron-sulfur flavoprotein trimethylamine dehydrogenase, *J. Biol. Chem. 263*, 3075–3078.
12. Scrutton, N. S. (1994) Alpha/Beta barrel evolution and the molecular assembly of enzymes: emerging trends in the flavin oxidase/dehydrogenase family, *Bioessays 16*, 115–122.
13. Wilson, E. K., Mathews, F. S., Packman, L. C. & Scrutton, N. S. (1995) Electron tunneling in substrate-reduced trimethylamine dehydrogenase: kinetics of electron transfer and analysis of the tunneling pathway, *Biochemistry 34*, 2584–2591.
14. Huang, L., Rohlfs, R. J. & Hille, R. (1995) The reaction of trimethylamine dehydrogenase with electron-transferring flavoprotein, *J. Biol. Chem. 270*, 23958–23965.
15. Klotz, I. M. (1946) The application of the law of mass action to binding by proteins: interactions with calcium, *Arch. Biochem. 9*, 109–117.
16. Kasprzak, A. A., Papas, E. J. & Steenkamp. D. J. (1983) Identity of the subunits and stoichiometry of prosthetic groups in trimethylamine dehydrogenase and dimethylamine dehydrogenase, *Biochem. J. 211*, 535–541.
17. Haschemeyer, R. H. & Bowers, W. F. (1970) Exponential analysis of concentration or concentration difference data for discrete molecular mass distributions in sedimentation equilibrium, *Biochemistry 9*, 435–445.
18. Milthorpe, B. K., Jeffreey, P. J. & Nichol, L. W. (1975) Direct analysis of sedimentation equilibrium results obtained with polymerizing systems, *Biophys. Chem. 3*, 169–176.
19. Wills, P. R. & Winzor, D. J. (1992) Thermodynamic nonideality and sedimentation equilibrium, in *Ultracentrifugation in biochemistry and polymer science* (Harding, S. E., Rowe, A. J. & Horton, J. C., eds) pp. 311–330, Royal Society Chemistry, Cambridge, UK.
20. Wills, P. R., Jacobsen, M. P. & Winzor, D. J. (1996) Direct analysis of solute self-association by sedimentation equilibrium, *Biopolymers 38*, 119–130.
21. Johnson, M. L. (1992) Why, when, and how biochemists should use least squares, *Anal. Biochem. 206*, 215–225.
22. Cölfen, H., Harding, S. E., Wilson, E. K., Scrutton, N. S. & Winzor, D. J. (1996) Low temperature solution behaviour of Methylophilus methylotrophus electron-transferring flavoprotein: a study by analytical ultracentrifugation, *Eur. Biophys. J., in the press.*
23. Cölfen, H., Harding, S. E., Wilson, E. K., Packman, E. C. & Scrutton, N. S. (1996) Homodimeric and expanded behaviour of trimethylamine dehydrogenase in solution at different temperatures, *Eur. Biophys. J. 24*, 159–164.
24. Nichol, L. W., Jeffrey, P. D. & Milthorpe, B. K. (1976) The sedimentation equilibrium of heterogeneously associating systems and mixtures of noninteracting solutes: analysis without determination of molecular mass averages, *Biophys. Chem. 4*, 259–267.
25. Van Holde, K. E. & Baldwin, R. L. (1958) Rapid attainment of sedimentation equilibrium, *J. Phys. Chem. 62*, 734–743.
26. Yphantis, D. A. (1964) Equilibrium ultracentrifugation of dilute solutions, *Biochemistry 3*, 297–317.
27. Jeffrey, P. D., Nichol, L. W. & Teasdale, R. D. (1979) Studies of macromolecular heterogeneous associations involving cross-linking: a re-examination of the ovalbumin-lysozyme system, *Biophys. Chem. 10*, 379–387.
28. Becerra, S. P., Kumar, A., Lewis, M. S., Widen, S. G., Abbotts, J., Karawya, E. M., Hughes, S. H., Shiloach, J. & Wilson, S. H. (1991) Protein-protein interactions of HIV-1 reverse transcriptase: implication of central and C-terminal regions in subunit binding, *Biochemistry 30*, 11707–11719.
29. Philo, J., Talvenheimo, J., Wen, J., Rosenfeld, R., Welcher, A. & Arakawa, T. (1994) Interactions of neurotrophin-3 (NT-3), brain-derived neurotrophic factor (BDNF), and the NT-3 · BDNF heterodimer of the TrkB and TrkC receptors, *J. Biol. Chem. 269*, 27840–27846.
30. Strickland, S., Palmer, G. & Massey, V. (1975) Determination of dissociation constants and specific rate constants of enzyme-substrate (or protein-ligand) interactions from rapid reaction kinetic data, *J. Biol. Chem. 250*, 4048–4052.